

# Conversion of CO<sub>2</sub> in Exhaust Gas to Formic Acid and Formamides with Wasted Silicon Recovered from End-of-Life Solar Panels

Ken Motokura,\* Yurino Sasaki, Yusuke Tanimura, Takuya Shiroshta, Shingo Hasegawa, Kousuke Arata, Ryoosuke Takemura, Kazuo Namba, and Yuichi Manaka



Cite This: *ACS Sustainable Resour. Manage.* 2025, 2, 1220–1227



Read Online

ACCESS |

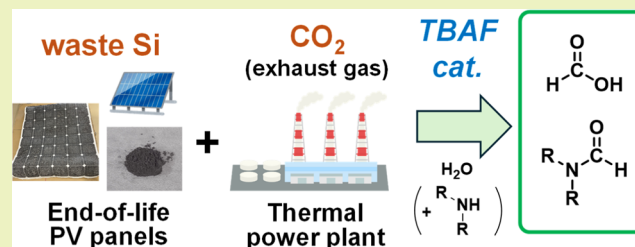
Metrics & More

Article Recommendations

Supporting Information

**ABSTRACT:** Recycling end-of-use solar panels faces significant challenges due to the high volume of discarded panels. The recycling of Si wafers recovered from these panels has drawn attention. In this study, we combined the recycling of waste silicon wafers with the conversion of CO<sub>2</sub> in exhaust gas from a thermal power plant. The reduction of CO<sub>2</sub> using silicon wafers as a reducing agent produced formic acid and formamides in high yields. The exhaust gas was directly introduced from the power plant to the reactor. The reactions were effective in the presence of a tetrabutylammonium fluoride catalyst. Among the four silicon samples recovered from solar panels, those with higher surface aluminum content showed lower reactivity; however, pretreatment with aqueous HCl significantly enhanced their reactivity. Detailed characterization of the Si samples before and after the reaction was conducted by using X-ray photoelectron spectroscopy, X-ray diffraction, scanning electron microscopy, and N<sub>2</sub> adsorption–desorption isotherms.

**KEYWORDS:** silicon, solar panel, carbon dioxide, exhaust gas, formic acid

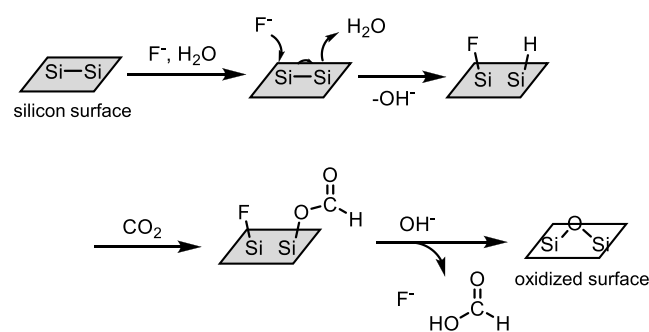


## INTRODUCTION

Solar panel recycling has gained attention due to the large volume of panels that will be discarded in the near future.<sup>1–4</sup> The International Renewable Energy Agency (IRENA) reported that by 2050, 60–78 MT of global photovoltaic (PV) panels will be discharged.<sup>5</sup> PV panels contain silicon wafers, accounting for approximately 2–3% of their weight.<sup>1</sup> The silicon wafer can be separated from the PV panel through physical and thermal processes during the end-of-use treatment. Recently, the recycling of waste Si has been actively studied.<sup>6–10</sup> For example, Bertau et al. reported recycling broken Si wafers with red mud to produce ferrosilicon alloys,<sup>6</sup> and Mathews et al. demonstrated the use of Si recovered from PV waste as electrodes in lithium-ion batteries.<sup>7</sup> However, there is no straightforward approach to use such wasted Si as a reducing agent of CO<sub>2</sub> for organic compounds.

Silicon-based compounds are an effective reducing agent for carbon resources, including carbon dioxide (CO<sub>2</sub>). The reduction of CO<sub>2</sub> to organic compounds is crucial for developing a carbon-neutral society.<sup>11–14</sup> Although the reaction between CO<sub>2</sub> and organosilicon compounds such as hydrosilane including polymethylhydrosiloxane as a byproduct of silicon industry is well-known,<sup>15–28</sup> reactions with metallic silicon are rare. Ozin et al. demonstrated CO<sub>2</sub> conversion to CO using hydride-terminated Si nanoparticles under light irradiation.<sup>29</sup> Dasog et al. reported methanol production from CO<sub>2</sub> by reaction with hydride-terminated porous silicon nanoparticles.<sup>30</sup> Both examples used freshly prepared Si

## Scheme 1. Reductive Reaction Pathway on the Silicon Surface



nanoparticles and large amounts of hydrofluoric acid. However, the reaction between metallic Si and CO<sub>2</sub> to form formic acid is thermodynamically favorable (eq 1). Thus, only a catalytic amount of the promoter is required to complete the reaction. Recently, our group reported the reduction of CO<sub>2</sub> to formic acid using a catalytic amount of fluoride salts at 95

**Received:** January 25, 2025

**Revised:** June 26, 2025

**Accepted:** June 26, 2025

**Published:** July 14, 2025





Figure 1. Concept of this research.

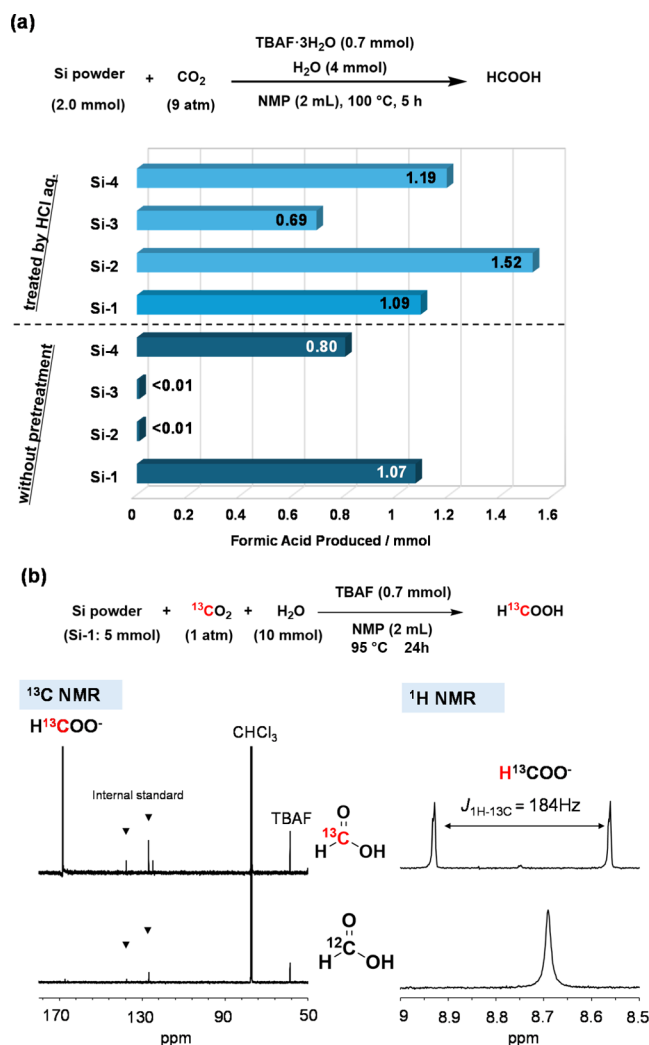
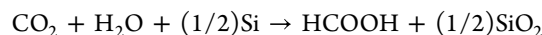


Figure 2. (a) Formic acid production from  $\text{CO}_2$  and waste silicon wafers (Si-1–4) with TBAF catalyst before and after aqueous HCl treatment. (b) Reaction of  $^{13}\text{CO}_2$  with waste silicon wafer (Si-1).  $^{13}\text{C}$  and  $^1\text{H}$  NMR of the reaction mixture.

$^\circ\text{C}$ .<sup>31–33</sup> This reaction system can be applied to crushed and milled silicon powder from fresh silicon wafers of PV panel preparation grade (Si > 99.9999%). The catalytic reaction pathway involves (i) surface Si–Si bond cleavage by fluoride

and  $\text{H}_2\text{O}$  as a proton source to give the Si–H species and (ii) reduction of  $\text{CO}_2$  to formate by the Si–H species (Scheme 1).<sup>31</sup> The in situ FT-IR analysis revealed that the reaction of silicon, fluoride, and proton afforded Si–H species on the powdered silicon surface.<sup>33</sup> The Si–Si bond cleavage process was also investigated by a homogeneous reaction system.<sup>22</sup>

In this study, we investigated the reactivity of waste silicon cells separated from end-of-use solar panels as reducing agents for  $\text{CO}_2$  to integrate recycle of both waste silicon and  $\text{CO}_2$  in exhaust gas. The separated silicon wafers were used for  $\text{CO}_2$  conversion after simple crushing and milling. The advantage of this reaction is that it does not require any form of discarded Si. The waste silicon cell contains a silver layer, silicon nitride layer, and other metals such as Al, Sn, and Cu with varying amounts in different samples. Among them, due to the presence of considerable Al, the effect of Al on the reactivity of four silicon samples was analyzed. The structure and composition of the silicon samples before and after reaction with  $\text{CO}_2$  were characterized to understand the reactivity of powdered silicon.



$$\Delta G^0 = -156 \text{ kJ/mol} \quad (1)$$

An important aspect of developing a  $\text{CO}_2$  conversion system is the use of real exhaust gas containing  $\text{CO}_2$ . We also investigated the reaction between waste silicon and exhaust gas from a thermal power plant containing 14 vol %  $\text{CO}_2$ . Formic acid was successfully obtained after the reduction of  $\text{CO}_2$  in exhaust gas using waste silicon as the reducing agent (Figure 1). Additionally, in the presence of amines, the corresponding formamide was formed as a product of the reductive conversion of  $\text{CO}_2$  (Figure 1).

## EXPERIMENTAL SECTION

**Materials.** Recovered silicon wafers from end-of-use solar panels were gifted by the solar panel recycling company. Four different silicon samples originated from different PV panels and separation process and were obtained, namely Si-1–4. The contents of trace metals in such silicon samples are summarized in Table S1. Tetrabutylammonium fluoride trihydrate ( $\text{TBAF}\cdot\text{3H}_2\text{O}$ , >99%) was purchased from Kanto Chemical, Co. Inc. without further purification.  $^{13}\text{CO}_2$  (99%) was purchased from Cambridge Isotope Laboratories. *N*-Methyl-2-pyrrolidone (NMP, dehydrated, >99%) was purchased from Kanto Chemical, Co. Inc. and used without further purification. Unless otherwise mentioned, all other materials were purchased from Tokyo Chemical Industry Co., Ltd., Kanto Chemical Co., Inc., and Aldrich Inc. Exhaust gas containing  $\text{CO}_2$  was supplied from the Isogo thermal power plant (coal-fired), Electric Power Development Co., Ltd.

**Analytical Methods.** The liquid  $^1\text{H}$  and  $^{13}\text{C}$  nuclear magnetic resonance (NMR) spectra were measured with  $\text{CDCl}_3$  as the solvent using the JEOL RESONANCE ECA 500 spectrometer (operating frequencies are 500 and 125 MHz for  $^1\text{H}$  and  $^{13}\text{C}$  NMR measurements, respectively) or ECX 400 (operating frequencies are 400 and 100 MHz for  $^1\text{H}$  and  $^{13}\text{C}$  NMR measurements, respectively). A Shimadzu QP2010 SE gas chromatograph-mass spectrometer (GC–MS) equipped with a DB-1 column and Shimadzu GC2025 gas chromatograph with flame ionization detection (GC–FID) were used for product characterization and/or quantification. Initially, the temperature was held at  $50^\circ\text{C}$  for 6 min, then raised with a rate of  $10^\circ\text{C}/\text{min}$  to  $280^\circ\text{C}$ , and then the temperature was held at  $280^\circ\text{C}$  for the final 10 min. X-ray photoelectron spectroscopy (XPS) analyses were performed on a ULVAC-PHI Quantera-SXM system equipped with an Al X-ray source. Spectra were obtained using a pass energy of 55.0 eV, and the Al  $K\alpha$  X-ray source was operated at 50.2 W and 14

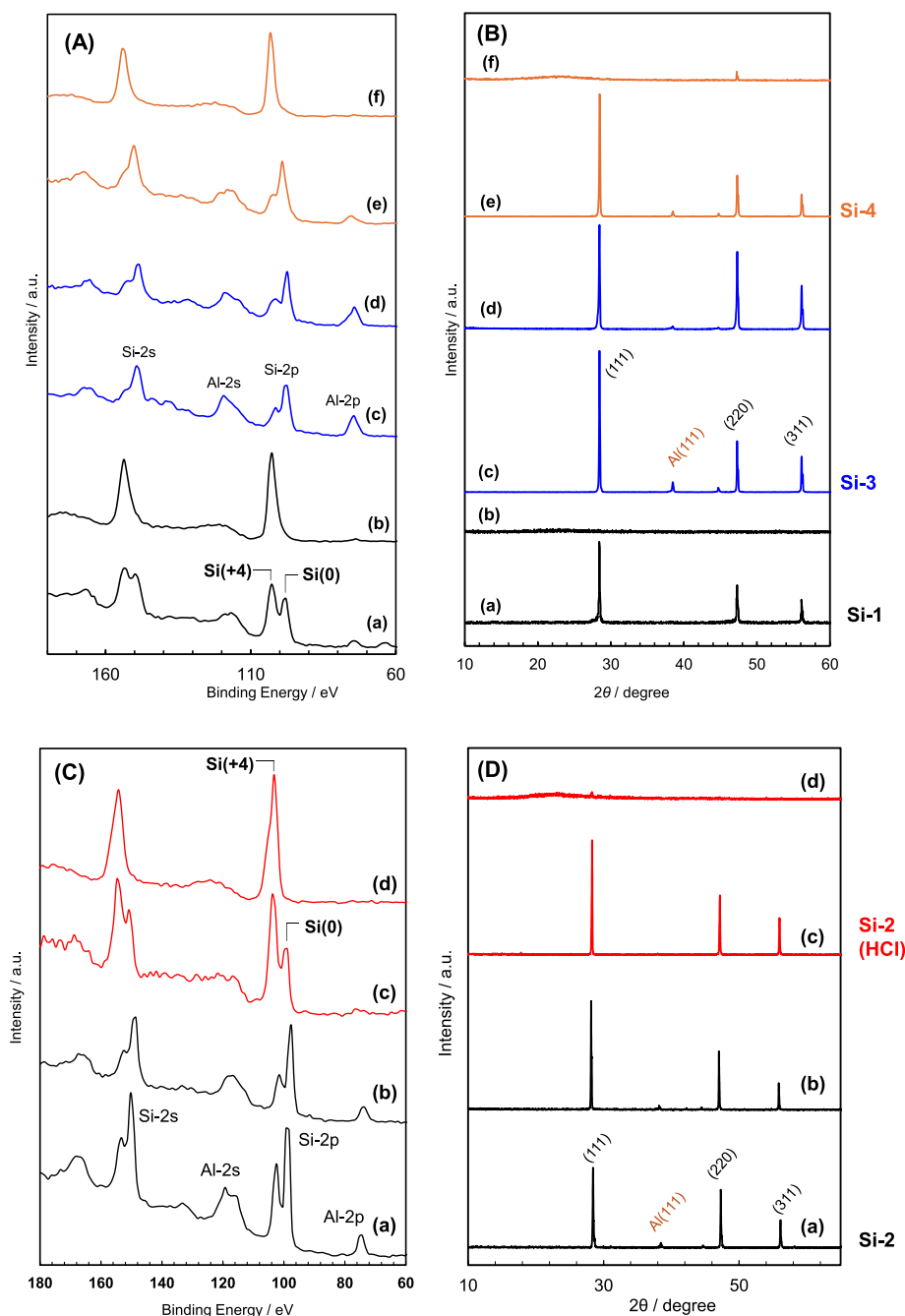


**Figure 3.** (A) XPS spectra and (B) XRD patterns of (a) Si-1, (b) recovered solid after the catalytic reaction with Si-1, (c) Si-3, (d) recovered solid after the catalytic reaction with Si-3, (e) Si-4, and (f) recovered solid after the catalytic reaction with Si-4. (C) XPS spectra and (D) XRD patterns of (a) Si-2, (b) recovered solid after the catalytic reaction with Si-2, (c) Si-2(HCl), and (d) recovered solid after the catalytic reaction with Si-2(HCl).

kV with a beam size of 200  $\mu\text{m}$ . Excess charges on the samples were neutralized by argon ion sputtering. The working pressure in the analysis chamber was less than  $1 \times 10^{-7}$  Pa. Spectra were acquired in the C 1s, Si 2p, and Al 2p regions. XPS element peaks were shifted to a C 1s position of 284.8 eV. Powder X-ray diffraction (XRD) patterns were recorded using a Rigaku Ultima IV diffractometer with  $\text{Cu K}\alpha$  radiation. Scanning electron microscopy (SEM) analysis of powdered silicon samples was performed by a QUANTA, FEG250.  $\text{N}_2$  adsorption–desorption isotherms at 77 K were measured using a BELSORP mini (MicrotracBEL) system. Samples were prepared for  $\text{N}_2$  adsorption measurements by outgassing at 473 K for 2 h under vacuum to a final pressure of 1 Pa. The BET surface areas were estimated over the relative pressure ( $P/P_0$ ) range of 0.30–0.70.

#### Preparation of Silicon Powder as the Reducing Agent.

Silicon wafers were crushed with alumina mortar to powdered form and sifted by an automatic sieve with a 40  $\mu\text{m}$  mesh size. The prepared silicon powders were stored in containers under an argon atmosphere tightly, and moisture was kept low by storing the container inside a desiccator. Several silicon samples were treated with aqueous HCl solution as follows: into a 35 wt % solution of HCl, 5.0 g of powdered silicon was added. The mixture was stored for 12 h at room temperature; then, the solid was filtered and washed with deionized water and acetone. The obtained solid was dried under vacuum and stored under an Ar atmosphere. The treated silicon is denoted as Si- $n$ (HCl).

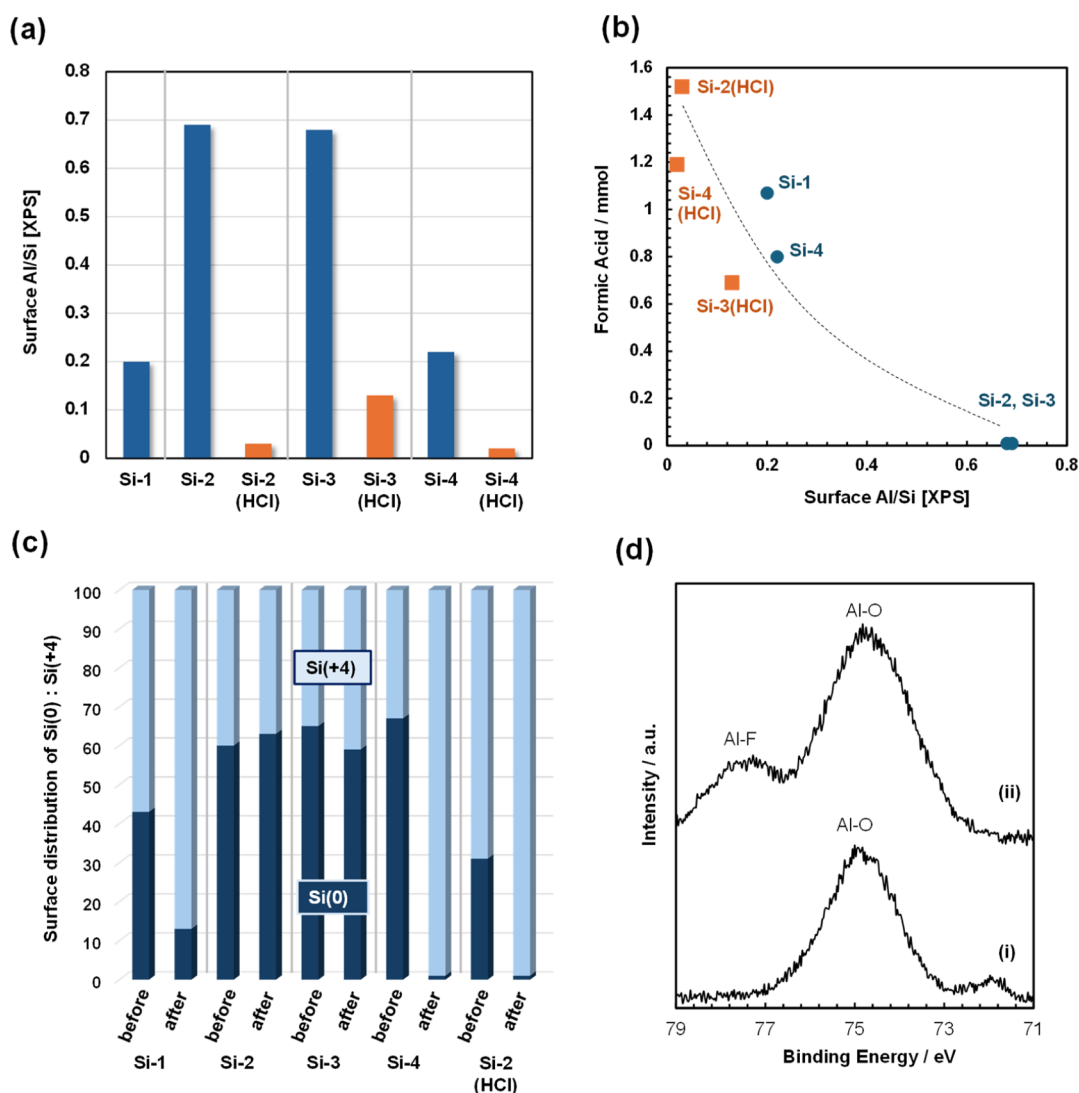


**Figure 4.** (a) Al/Si ratio of powdered silicon samples recovered from end-of-life solar cells. (b) Effect of the Al/Si ratio of silicon, determined by XPS, on the yield of formic acid in the reduction of CO<sub>2</sub>. (c) Si(0):Si(+4) distribution of powdered silicon samples before and after the catalytic reaction, determined by XPS. (d) Al-2p XPS spectra of (a) parent Si-3 and (b) recovered solid after the catalytic reaction with Si-3.

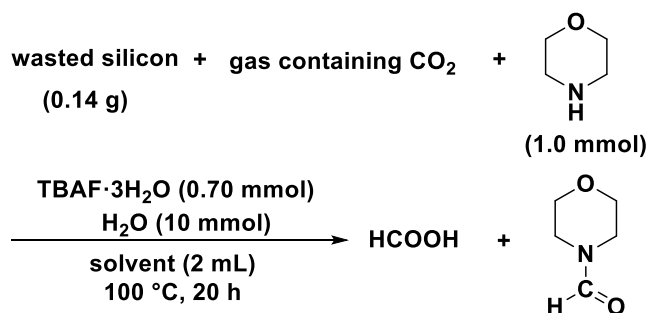
**Table 1. Formic Acid Production from Waste Silicon Cells and CO<sub>2</sub><sup>a</sup>**

| entry | gas (vol % content)   | CO <sub>2</sub> (atm)/total (atm) | x (Si/mg)/y (TBAF/mmol) | formic acid yield/mmol |
|-------|---|-----------------------------------|-------------------------|------------------------|
| 1     | CO <sub>2</sub> (100)   | 1.0/1.0                           | 56/0.70                 | 0.66                   |
| 2     | CO <sub>2</sub> (14.3) + N <sub>2</sub> (bal.)  | 1.3/9.0                           | 56/0.70                 | 0.79 <sup>b</sup>      |
| 3     | CO <sub>2</sub> (14.2) + O <sub>2</sub> (5.1) + N <sub>2</sub> (bal.)   | 1.3/9.0                           | 56/0.70                 | 0.39                   |
| 4     | CO <sub>2</sub> (14.2) + O <sub>2</sub> (5.1) + N <sub>2</sub> (bal.)   | 1.3/9.0                           | 56/0.70                 | 0.40 <sup>b</sup>      |
| 5     | exhaust gas from thermal power plant [CO <sub>2</sub> (14) + O <sub>2</sub> (5) + N <sub>2</sub> (bal.)] <sup>c</sup> | 1.3/9.0                           | 56/0.70                 | 0.53                   |
| 6     | exhaust gas from thermal power plant [CO <sub>2</sub> (14) + O <sub>2</sub> (5) + N <sub>2</sub> (bal.)] <sup>c</sup> | 1.3/9.0                           | 140/0.70                | 0.85                   |
| 7     | exhaust gas from thermal power plant [CO <sub>2</sub> (14) + O <sub>2</sub> (5) + N <sub>2</sub> (bal.)] <sup>c</sup> | 1.3/9.0                           | 140/1.0                 | 1.10                   |
| 8     | exhaust gas from thermal power plant [CO <sub>2</sub> (14) + O <sub>2</sub> (5) + N <sub>2</sub> (bal.)] <sup>c</sup> | 1.3/9.0                           | 140/0.70                | 0.78 <sup>d</sup>      |

<sup>a</sup>Reaction conditions: Si-2 treated with HCl aq. (*x* mg), NMP (2 mL), TBAF·3H<sub>2</sub>O (*y* mmol), gas containing CO<sub>2</sub>, 100 °C, 24 h. Yields are determined by <sup>1</sup>H NMR by an internal standard technique. <sup>b</sup>120 °C. <sup>c</sup>Exhaust gas from thermal power plant (CO<sub>2</sub>: 14 vol %; O<sub>2</sub>: 5 vol %; N<sub>2</sub>: bal.; NO<sub>x</sub>: 8 ppm, and SO<sub>x</sub>: lower than ppm level). <sup>d</sup>Exhaust gas was directly charged to a reactor from the thermal power plant (Figure 6b).

**Typical Procedure for Fluoride-Catalyzed CO<sub>2</sub> Reduction with Wasted Silicon Powder and H<sub>2</sub>O.** A SUS autoclave was used as a reactor. To the reactor was added 2.0 mmol powdered silicon

wafer (0.056 g) was added. In a vial, catalyst (typically TBAF·3H<sub>2</sub>O, 0.70 mmol), solvent (typically NMP, 2 mL), and a definite amount of deionized water (typically 4 mmol) were mixed and introduced to the

Table 2. Formamide Synthesis from Morpholine, Waste Silicon Cells, and CO<sub>2</sub><sup>a</sup>

| gas (vol % content)   | CO <sub>2</sub> (atm)/total (atm) | formic acid yield/mmol | amide yield/mmol  |
|---|-----------------------------------|------------------------|-------------------|
| CO <sub>2</sub> (100)   | 9.0/9.0                           | 1.10                   | 0.76              |
| exhaust gas from thermal power plant [CO <sub>2</sub> (14) + O <sub>2</sub> (5) + N <sub>2</sub> (bal.)] <sup>b</sup> | 1.3/9.0                           | 0.31                   | 0.46              |
| exhaust gas from thermal power plant [CO <sub>2</sub> (14) + O <sub>2</sub> (5) + N <sub>2</sub> (bal.)] <sup>b</sup> | 1.3/9.0                           | 0.40                   | 0.38 <sup>c</sup> |

<sup>a</sup>Reaction conditions: Si-2(HCl) (0.14 g), NMP (2 mL), TBAF·3H<sub>2</sub>O (0.70 mmol), H<sub>2</sub>O (10 mmol), and gas containing CO<sub>2</sub>, 100 °C, 24 h. Yields were determined by <sup>1</sup>H NMR spectroscopy using an internal standard technique. <sup>b</sup>Exhaust gas from a thermal power plant (collected in a cylinder, CO<sub>2</sub>: 14 vol %; O<sub>2</sub>: 5 vol %; N<sub>2</sub>: balance, NO<sub>x</sub>: 8 ppm, and SO<sub>x</sub>: lower than ppm level). <sup>c</sup>Exhaust gas was directly charged into the reactor from a thermal power plant (Figure 6b).

reactor. Afterward, reaction gas (typically, CO<sub>2</sub>, 9 atm) was introduced. The resulting mixture was stirred vigorously at 100 °C for 24 h. The reaction products were confirmed by <sup>1</sup>H NMR spectrometry. The formic acid yield was determined by liquid <sup>1</sup>H NMR in CDCl<sub>3</sub> solvent using an internal standard technique with 1,3,5-triisopropylbenzene as the internal standard. The quantitative correlation of the <sup>1</sup>H NMR peak area of formic acid and the internal standard (triisopropylbenzene) was confirmed by standard samples.

## RESULTS AND DISCUSSION

**Reduction of CO<sub>2</sub> to Formic Acid with Wasted Silicon Wafer.** The reduction of CO<sub>2</sub> to formic acid with waste silicon wafers was studied. Waste Si samples, supplied by a solar panel recycling company, were separated from different end-of-life solar panels and tested as reducing agents of CO<sub>2</sub>. The waste Si samples were crushed and milled in an alumina mortar, and the powdered Si was used for the CO<sub>2</sub> reduction. The reaction was initially conducted under 9 atm of pure CO<sub>2</sub> TBAF in NMP for 5 h at 100 °C. The results are summarized in Figure 2a. Without pretreatment of silicon powder, samples Si-1 and Si-4 showed reactivity, yielding 1.25 and 0.80 mmol formic acid, respectively. In contrast, Si-2 and Si-3 were unreactive and no formic acid was detected. These results indicate that the reactivity of waste Si is highly dependent on the sample. Notably, the reactivity of Si significantly increased after treatment with an aqueous HCl solution before the catalytic reaction, and formic acid production was then detected for Si-2 and Si-3 (Figure 2a). Si-2(HCl) produced the largest amount of formic acid (1.52 mmol). Theoretically, 2 mmol formic acid is formed from 1 mmol Si. Therefore, the yield based on Si in the reaction with Si-2(HCl) was 38%. The formic acid yield based on Si is summarized in Table S1, Supporting Information.

Formate exclusively originated from CO<sub>2</sub> as confirmed through isotopic experiments using <sup>13</sup>CO<sub>2</sub>, as shown in Figure 2b. After the reaction, the mixture was dissolved in CDCl<sub>3</sub>, and <sup>1</sup>H/<sup>13</sup>C NMR measurements were conducted. A significant increase in the signal at 168 ppm, assigned to the formyl carbon, was detected in the <sup>13</sup>C NMR spectrum. Additionally, doublet peaks centered at 8.75 ppm with *J* = 184 Hz were detected in the <sup>1</sup>H NMR spectrum, indicating <sup>1</sup>H-<sup>13</sup>C

coupling.<sup>34</sup> These results clearly indicate the conversion of CO<sub>2</sub> to formic acid.

XPS and XRD analyses of the waste silicon powder were conducted to analyze the structural changes in silicon before and after the catalytic reaction in a CO<sub>2</sub> atmosphere (Figure 3). The results for Si-1, Si-3, and Si-4 are shown in Figure 3A,B. For Si-1 (a, b) and Si-4 (e, f), the XPS signal assigned to Si(0) (98 eV) disappeared after the reaction (b, f), and only the Si(+4) peak at 103 eV was detected around the Si-2p region (Figure 3A). The Si(+4) signal is assigned to oxidized Si (SiO<sub>2</sub>) and a small amount of silicon nitride. In contrast, no significant spectral changes were detected for Si-3 (Figure 3A, c,d). As shown in the XRD patterns, the signals arising from the Si crystals disappeared after the reaction in the cases of Si-1 (a, b) and Si-4 (e, f), whereas no significant change was detected in Si-3 (c, d) (Figure 3B). As shown in Figure 3C,D, the Si-2 sample exhibited similar phenomena to Si-3; no significant XPS or XRD changes were observed after the reaction (a, b). These spectral trends correspond to the catalytic reaction results. The zerovalent Si crystals in the reactive Si (Si-1 and Si-4) react with CO<sub>2</sub> to form formic acid and SiO<sub>2</sub>. Notably, Si with low reactivity (Si-2 and Si-3) contained considerable amounts of Al: Al-2p/2s signals were detected by XPS, and Al(111) diffraction was observed in the XRD pattern. Therefore, it was suggested that Al suppresses the reductive conversion of CO<sub>2</sub> to formic acid.

The XPS and XRD results for Si-2 with and without HCl treatment are shown in Figure 3C,D. After treatment, the Al signals almost disappeared in both the XPS and XRD analyses (Figure 3C(c),D(c)). The surface Al/Si ratios determined by XPS are shown in Figure 4a. After treatment, the Al/Si ratio decreased significantly in all three samples (Si-2, Si-3, and Si-4). Thus, the treatment of Si with aqueous HCl is an effective method for removing surface Al species. Additionally, the Al/Si ratio before treatment indicated that the low-Al-content samples (Si-1 and Si-4) exhibited good reactivity with CO<sub>2</sub>, as shown in Figure 1a. After HCl treatment, all Si samples showed a high reactivity with CO<sub>2</sub> (Figure 1a). Figure 4b shows the effect of the Al/Si surface ratio on the amount of formic acid. This relationship clearly indicates that the presence of Al decreased the reactivity of silicon powder.

The presence of other trace metals, such as Cu and Sn, was detected in silicon samples (Table S1, Supporting Information), however, there is no correlation between the content of such trace metals and silicon reactivity. The surface area of silicon samples ( $15\text{--}1\text{ m}^2\text{ g}^{-1}$ ) also indicates that there is no significant effect of silicon morphology on its reactivity (Table S2, Supporting Information). Figure 4c summarizes the Si(0)/Si(+4) distribution of the powdered Si surface determined by Si-2p XPS deconvolution spectra (Figures S1–5). The amount of zerovalent Si significantly decreased after the catalytic reaction in highly reactive Si samples Si-1, Si-4, and Si-2(HCl), indicating that the reduction of CO<sub>2</sub> with Si(0) species occurred in these samples. Figure 4d shows the Al-2p XPS spectra of the parent Si-3 sample before and after the catalytic reaction. No CO<sub>2</sub> conversion was observed for parent Si-3. After the reaction, a new signal assigned to Al–F was detected at 77.4 eV.

The fluoride anion of TBAF likely reacts with the Al species and is fixed on the surface in the Al–F form. This could be the primary reason for the low or no reactivity of silicon powders containing substantial amounts of Al (Si-2 and Si-3) in CO<sub>2</sub> conversion reactions. XPS and XRD analyses of the silicon powders Si-1 and Si-2(HCl) after the catalytic reaction showed no signal assigned to the silicon crystal (Figure 3B(b),D(d)), suggesting the oxidation of the whole part of the silicon

particles. SEM images of powdered Si before and after the reaction with CO<sub>2</sub> are shown in Figure 5. After the reaction, the crystal structure changed to aggregated small fine particles (Figure 5B,D). Brunauer–Emmett–Teller (BET) analysis of the silicon powder also indicated a significant increase in the surface area of the recovered silicon particles after the catalytic reaction (Figure 5E). Similar phenomena were also observed in the case of pure silicon powder.<sup>32,33</sup> These results clearly show that not only Si(0) atoms on the surface but also the interior of the silicon powder were consumed as the reductant for CO<sub>2</sub>, leading to efficient conversion of CO<sub>2</sub> to formic acid.

**Reduction of CO<sub>2</sub> in Exhaust Gas with Wasted Silicon Wafer.** Next, the reaction between waste silicon and CO<sub>2</sub> in simulated and actual exhaust gases was investigated. Table 1 summarizes the results of the CO<sub>2</sub> reduction using Si-2(HCl). Several concentrations of CO<sub>2</sub> and O<sub>2</sub> were tested. When using a gas containing 14.3 vol % of CO<sub>2</sub> with a N<sub>2</sub> balance, 0.79 mmol formic acid was detected at a total gas pressure and CO<sub>2</sub> partial pressure of 9.0 and 1.3 atm, respectively (entry 2). This result is close to the result of 1.0 atm of pure CO<sub>2</sub> (entry 1). The amount of formic acid slightly decreased when a simulated exhaust gas containing both CO<sub>2</sub> (14.2 vol %) and O<sub>2</sub> (5.1 vol %) was used: approximately 0.40 mmol formic acid was formed (entries 3 and 4). Subsequently, the exhaust gas was

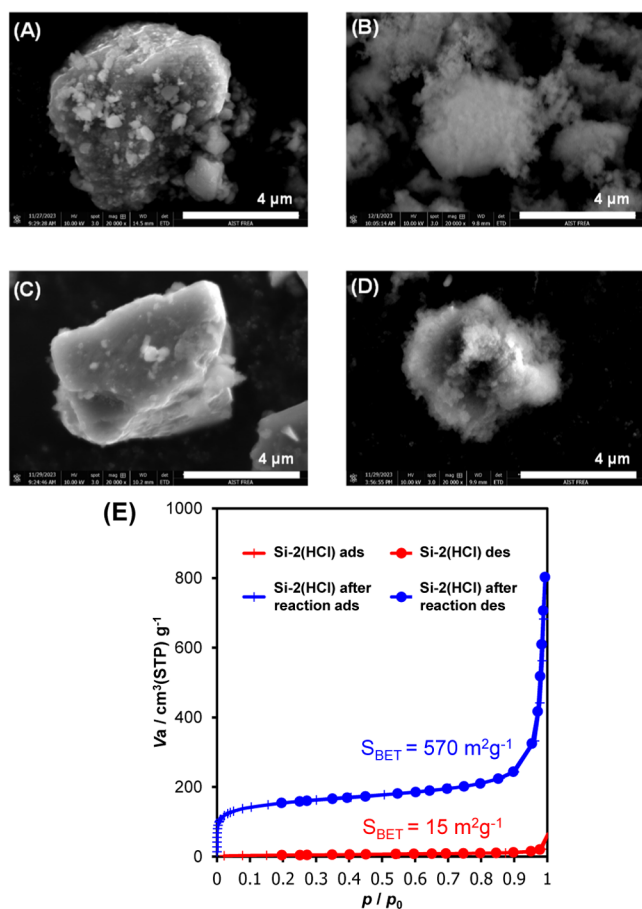


**Figure 5.** SEM images of (A) powdered Si-1, (B) recovered powder after the catalytic reaction with Si-1, (C) powdered Si-2(HCl), (D) recovered powder after the catalytic reaction with Si-2(HCl), and (E) N<sub>2</sub> adsorption–desorption isotherm/surface area ( $S_{\text{BET}}$ ) of powdered Si-2(HCl) and recovered sample after the catalytic reaction.

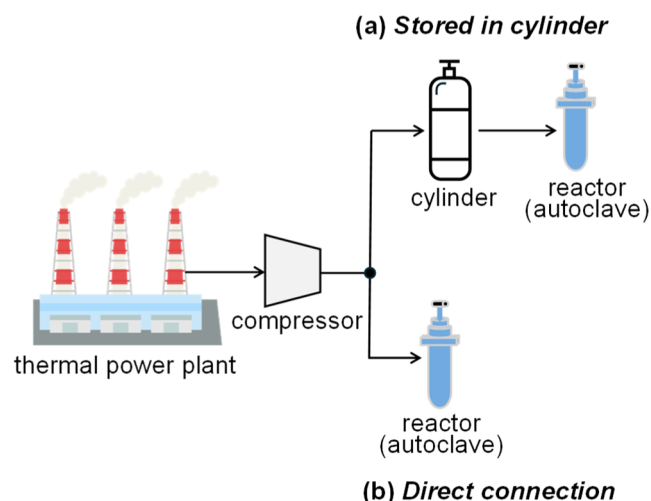


**Figure 6.** Sampling of exhaust gas from a thermal power plant. (a) Gas storage in a cylinder and (b) direct connection of the reactor to the exhaust port of the thermal power plant.

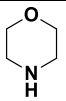
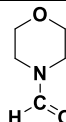
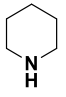
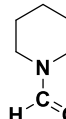
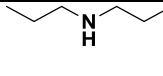
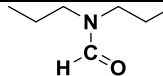
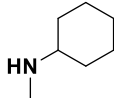
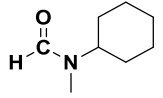
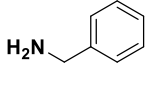
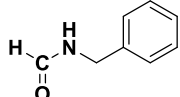
collected at a thermal power plant by using a gas cylinder, as shown in Figure 6a. The collected gas was pressurized using a compressor, and the actual exhaust gas also reacted to produce formic acid (entries 5–7). Increasing the amount of silicon and TBAF increased the formic acid yield to 1.10 mmol with a 73% yield based on the amount of CO<sub>2</sub> loaded in the reactor (entry 7). Additionally, the exhaust gas can be collected directly from the exhaust port of the thermal power plant into the reactor by using a compressor (Figure 6b). In this case, a similar formic acid yield was detected (entry 8). Overall, the presence of O<sub>2</sub> slightly affected the reaction, and the presence of very small amounts of NO<sub>x</sub> and SO<sub>x</sub> in the exhaust gas did not affect the reduction of the level of CO<sub>2</sub>. This is the first report of the production of formic acid from waste Si and CO<sub>2</sub> in exhaust gases.

The addition of an amine to the CO<sub>2</sub> reduction system using a silicon reducing agent enabled formamide production.<sup>33</sup> The formation of *N*-formyl morpholine was detected in the reaction

**Table 3. Scope of Amine in Formamide Synthesis with Waste Silicon Cells and Exhaust Gas from Thermal Power Plant<sup>a</sup>**

$$\text{wasted silicon (0.14 g)} + \text{exhaust gas from thermal power plant (9 atm)} + \begin{matrix} \text{R}-\text{N}-\text{R} \\ | \\ \text{H} \end{matrix} \text{ (1.0 mmol)}$$

$$\xrightarrow[\text{NMP (2 mL), 160 }^\circ\text{C, 16 h}]{\text{TBAF}\cdot\text{3H}_2\text{O (0.70 mmol), H}_2\text{O (10 mmol)}} \text{HCOOH} + \begin{matrix} \text{R}-\text{N}-\text{R} \\ | \\ \text{H}-\text{C}=\text{O} \end{matrix}$$

| Amine Substrate   | Formamide Product   | Formic acid yield / mmol | Formamide yield / % <sup>b</sup> |
|---|---|--------------------------|----------------------------------|
|    |    | 0.06                     | 75                               |
|   |   | <0.01                    | 61                               |
|  |  | 0.09                     | 31                               |
|  |  | 0.09                     | 27                               |
|  |  | <0.01                    | 47                               |

<sup>a</sup>Reaction conditions: Si-2(HCl) (0.14 g), NMP (2 mL), TBAF·3H<sub>2</sub>O (0.70 mmol), H<sub>2</sub>O (10 mmol), exhaust gas from thermal power plant (collected in a cylinder, total pressure: 9 atm; CO<sub>2</sub>: 14 vol %; O<sub>2</sub>: 5 vol %; N<sub>2</sub>: balance; NO<sub>x</sub>: 8 ppm, and SO<sub>x</sub>: lower than ppm level), 160 °C, 16 h. Yields determined by <sup>1</sup>H NMR using an internal standard technique. The formamide yield depends on the amine used.  
<sup>b</sup>Yields based on the amines used.

of waste silicon, CO<sub>2</sub> in the exhaust gas, and morpholine (Table 2). After the conditions were optimized, the yield of *N*-formyl morpholine increased to 75%, as shown in Table 3. Other secondary and primary amines, such as piperidine and benzylamine, were also examined in the presence of waste silicon and exhaust gases (Table 3). In all cases, the formation of the corresponding formamide was confirmed with 27–61% yields based on the amine used.

## CONCLUSION

Waste silicon wafers recovered from end-of-use solar panels were utilized as reducing agents for CO<sub>2</sub>. CO<sub>2</sub> in exhaust gas from a thermal power plant was successfully converted into formic acid through a reaction with waste silicon powder,

water, and TBAF. Si samples with higher Al content showed much lower reactivity, whereas treatment with an aqueous HCl solution effectively removed Al, resulting in high reactivity with CO<sub>2</sub> to produce formic acid. XPS suggested the poisoning of the fluoride catalyst by Al. The yield of formic acid based on the CO<sub>2</sub> in exhaust gas reached 73%. In the presence of amines, the formamide product was selectively formed from CO<sub>2</sub> and silicon powder in good-to-high yields. The surface and bulk characteristics of silicon powder before and after the catalytic reaction were analyzed by XPS, XRD, SEM, and N<sub>2</sub> adsorption–desorption measurements. XPS analysis revealed that the surface Si(0) species reacted with CO<sub>2</sub> and was then oxidized to Si(+4). XRD, SEM, and N<sub>2</sub> adsorption–desorption analyses indicated that both the surface and interior of the silicon powder reacted with CO<sub>2</sub>, suggesting a highly efficient CO<sub>2</sub> conversion reaction. The successful direct connection of the reactor to the exhaust gas port at the thermal power plant demonstrates the high potential for developing an actual process for the effective utilization of both waste silicon wafers and emitted CO<sub>2</sub>. This research is the first example of the integration of recycling of waste silicon wafers from end-of-life solar panels with the conversion of CO<sub>2</sub> in the exhaust gas.

## ASSOCIATED CONTENT

### Supporting Information

The Supporting Information is available free of charge at <https://pubs.acs.org/doi/10.1021/acssusresmgt.5c00056>.

Experimental details, results of elemental analysis, additional data of catalytic reactions, and XPS deconvolution spectra (PDF)

## AUTHOR INFORMATION

### Corresponding Author

Ken Motokura – Department of Chemistry and Life Science, Yokohama National University, Yokohama 240-8501, Japan; [orcid.org/0000-0002-0066-5139](https://orcid.org/0000-0002-0066-5139); Email: [motokura-ken-xw@ynu.ac.jp](mailto:motokura-ken-xw@ynu.ac.jp)

### Authors

Yurino Sasaki – Department of Chemistry and Life Science, Yokohama National University, Yokohama 240-8501, Japan  
Yusuke Tanimura – Department of Chemistry and Life Science, Yokohama National University, Yokohama 240-8501, Japan  
Takuya Shiroshta – Department of Chemistry and Life Science, Yokohama National University, Yokohama 240-8501, Japan  
Shingo Hasegawa – Department of Chemistry and Life Science, Yokohama National University, Yokohama 240-8501, Japan; [orcid.org/0000-0001-5295-017X](https://orcid.org/0000-0001-5295-017X)  
Kousuke Arata – Electric Power Development Co., Ltd., Kitakyushu 808-0111, Japan  
Ryosuke Takemura – Electric Power Development Co., Ltd., Kitakyushu 808-0111, Japan  
Kazuo Namba – Electric Power Development Co., Ltd., Kitakyushu 808-0111, Japan  
Yuichi Manaka – Renewable Energy Research Center, National Institute of Advanced Industrial Science and Technology (AIST), Koriyama, Fukushima 963-0298, Japan; [orcid.org/0000-0001-5872-3365](https://orcid.org/0000-0001-5872-3365)

Complete contact information is available at: <https://pubs.acs.org/doi/10.1021/acssusresmgt.5c00056>

## Notes

The authors declare no competing financial interest.

## ACKNOWLEDGMENTS

This research was financially supported by the JST-ALCA-Next Japan Grant Number JPMJAN23C7, the JSPS KAKENHI (Grant No. 23K23131), and the Carbon Recycling Fund Institute.

## REFERENCES

- (1) Peplow, M. Solar Panels Face Recycling Challenge. *ACS Cent. Sci.* **2022**, *8* (3), 299–302.
- (2) Klugmann-Radziemska, E.; Kuczyn'ska-Lazewska, A. The use of recycled semiconductor material in crystalline silicon photovoltaic modules production - A life cycle assessment of environmental impacts. *Sol. Energy Mater. Sol. Cells* **2020**, *205*, 110259.
- (3) Preet, S.; Smith, S. T. A comprehensive review on the recycling technology of silicon based photovoltaic solar panels: Challenges and future outlook. *J. Clean. Prod.* **2024**, *448*, 141661.
- (4) Gahlot, R.; Mir, S.; Dhawan, N. Recycling of Discarded Photovoltaic Solar Modules for Metal Recovery: A Review and Outlook for the Future. *Energy Fuels* **2022**, *36* (24), 14554–14572.
- (5) Weckend, S.; Wade, A.; Heath, G. A. *End of Life Management Solar Photovoltaic Panels*; IRENA And IEA-PVPS, 2016. <https://www.irena.org/publications/2016/Jun/End-of-life-management-Solar-Photovoltaic-Panels>.
- (6) Blaesing, L.; Walnsch, A.; Hippmann, S.; Modrzynski, C.; Weidlich, C.; Pavón, S.; Bertau, M. Ferrosilicon Production from Silicon Wafer Breakage and Red Mud. *ACS Sustainable Resour. Manage.* **2024**, *1* (3), 404–416.
- (7) Sim, Y.; Tay, Y. B.; Ankit; Lin, X.; Mathews, N. Simplified silicon recovery from photovoltaic waste enables high performance, sustainable lithium-ion batteries. *Sol. Energy Mater. Sol. Cells* **2023**, *257*, 112394.
- (8) Gao, X.; He, R.; Du, J.; Zhou, D.; Chen, A.; Sun, X. Recycling Solar Cells for Hydrogen Production Coupling Hydrazine Degradation with Entropy-Driven High-Chaos Nickel Molybdenum Phosphorus Sulfide Oxides. *ACS Catal.* **2022**, *12* (22), 14387–14397.
- (9) Wang, O.; Chen, Z.; Ma, X. Advancing sustainable end-of-life strategies for photovoltaic modules with silicon reclamation for lithium-ion battery anodes. *Green Chem.* **2024**, *26* (7), 3688–3697.
- (10) Shin, J.; Park, J.; Park, N. A method to recycle silicon wafer from end-of-life photovoltaic module and solar panels by using recycled silicon wafers. *Sol. Energy Mater. Sol. Cells* **2017**, *162*, 1–6.
- (11) Aresta, M. *Carbon Dioxide as Chemical Feedstock*; Wiley: Weinheim, 2010.
- (12) Wang, W.-H.; Feng, X.; Bao, M. *Transformation of Carbon Dioxide to Formic Acid and Methanol*; Wang, W.-H., Feng, X., Bao, M., Eds.; Springer: Singapore, 2018; pp 1–6.
- (13) Sakakura, T.; Choi, J. C.; Yasuda, H. Transformation of Carbon Dioxide. *Chem. Rev.* **2007**, *107*, 2365–2387.
- (14) De Luna, P.; Hahn, C.; Higgins, D.; Jaffer, S. A.; Jaramillo, T. F.; Sargent, E. H. What would it take for renewably powered electro-synthesis to displace petrochemical processes? *Science* **2019**, *364*, 350.
- (15) Liu, Q.; Wu, L.; Jackstell, R.; Beller, M. Using carbon dioxide as a building block in organic synthesis. *Nat. Commun.* **2015**, *6*, 5933.
- (16) Fernández-Alvarez, F. J.; Aitani, A. M.; Oro, L. A. Homogeneous catalytic reduction of CO<sub>2</sub> with hydrosilanes. *Catal. Sci. Technol.* **2014**, *4*, 611–624.
- (17) Iglesias, M.; Fernández-Alvarez, F. J.; Oro, L. A. Non-classical hydrosilane mediated reductions promoted by transition metal complexes. *Coord. Chem. Rev.* **2019**, *386*, 240–266.
- (18) Takaya, J.; Iwasawa, N. Synthesis, Structure, and Catalysis of Palladium Complexes Bearing a Group 13 Metalloligand: Remarkable Effect of an Aluminum-Metalloligand in Hydrosilylation of CO<sub>2</sub>. *J. Am. Chem. Soc.* **2017**, *139*, 6074–6077.
- (19) Fiorani, G.; Guo, W.; Kleij, A. W. Sustainable conversion of carbon dioxide: the advent of organocatalysis. *Green Chem.* **2015**, *17*, 1375–1389.
- (20) Liu, X.-F.; Ma, R.; Qiao, C.; Cao, H.; He, L.-N. Fluoride-Catalyzed Methylation of Amines by Reductive Functionalization of CO<sub>2</sub> with Hydrosilanes. *Chem.—Eur. J.* **2016**, *22*, 16489–16493.
- (21) Bobbink, F. D.; Das, S.; Dyson, P. J. *N*-formylation and *N*-methylation of amines using metal-free *N*-heterocyclic carbene catalysts and CO<sub>2</sub> as carbon source. *Nat. Protoc.* **2017**, *12*, 417–428.
- (22) Motokura, K.; Najjo, M.; Yamaguchi, S.; Miyaji, A.; Baba, T. Silicone Wastes as Reducing Agents for Carbon Dioxide Transformation: Fluoride-catalyzed Formic Acid Synthesis from CO<sub>2</sub>, H<sub>2</sub>O, and Disilanes. *Chem. Lett.* **2015**, *44*, 1464–1466.
- (23) Motokura, K.; Nakagawa, C.; Pramudita, R. A.; Manaka, Y. Formate-Catalyzed Selective Reduction of Carbon Dioxide to Formate Products Using Hydrosilanes. *ACS Sustainable Chem. Eng.* **2019**, *7*, 11056–11061.
- (24) Pramudita, R. A.; Manaka, Y.; Motokura, K. A Resin-Supported Formate Catalyst for the Transformative Reduction of Carbon Dioxide with Hydrosilanes. *Chem.—Eur. J.* **2020**, *26*, 7937–7945.
- (25) Pramudita, R. A.; Motokura, K. Transformative reduction of carbon dioxide through organocatalysis with silanes. *Green Chem.* **2018**, *20*, 4834–4843.
- (26) Pramudita, R. A.; Motokura, K. Heterogeneous Organocatalysts for the Reduction of Carbon Dioxide with Silanes. *ChemSusChem* **2021**, *14*, 281–292.
- (27) Pramudita, R. A.; Motokura, K. Efficient Conversion of Carbon Dioxide with Si-based Reducing Agents Catalyzed by Metal Complexes and Salts. *Chem. Rec.* **2019**, *19*, 1199–1209.
- (28) Li, X.-Y.; Zheng, S.-S.; Liu, X.-F.; Yang, Z.-W.; Tan, T.-Y.; Yu, A.; He, L.-N. Waste Recycling: Ionic Liquid-Catalyzed 4-Electron Reduction of CO<sub>2</sub> with Amines and Polymethylhydrosiloxane Combining Experimental and Theoretical Study. *ACS Sustainable Chem. Eng.* **2018**, *6*, 8130–8135.
- (29) Sun, W.; Qian, C.; He, L.; Ghuman, K. K.; Wong, A. P.; Jia, J.; Ali, F. M.; O'Brien, P. G.; Reyes, L. M.; Wood, T. E.; Helmy, A. S.; Mims, C. A.; Singh, C. V.; Ozin, G. A. Heterogeneous reduction of carbon dioxide by hydride-terminated silicon nanocrystals. *Nat. Commun.* **2016**, *7*, 12553.
- (30) Dasog, M.; Kraus, S.; Sinelnikov, R.; Veinot, J. G.; Rieger, B. CO<sub>2</sub> to methanol conversion using hydride terminated porous silicon nanoparticles. *Chem. Commun.* **2017**, *53* (21), 3114–3117.
- (31) Pramudita, R. A.; Nakao, K.; Nakagawa, C.; Wang, R.; Mochizuki, T.; Takato, H.; Manaka, Y.; Motokura, K. Catalytic reduction and reductive functionalisation of carbon dioxide with waste silicon from solar panel as the reducing agent. *Energy Adv.* **2022**, *1* (6), 385–390.
- (32) Motokura, K.; Nakao, K.; Manaka, Y. Fluoride Catalysts and Organic Additives for Conversion of CO<sub>2</sub> to Formic Acid and Methanol using Powdered Silicon as Reducing Agent. *Asian J. Org. Chem.* **2022**, *11* (10), No. e202200230.
- (33) Wang, R.; Nakao, K.; Manaka, Y.; Motokura, K. CO<sub>2</sub> conversion to formamide using a fluoride catalyst and metallic silicon as a reducing agent. *Commun. Chem.* **2022**, *5* (1), 150.
- (34) Tamaki, Y.; Koike, K.; Ishitani, O. Highly efficient, selective, and durable photocatalytic system for CO<sub>2</sub> reduction to formic acid. *Chem. Sci.* **2015**, *6*, 7213–7221.